Chemisorption of Hydrogen Atoms on the Sidewalls of Armchair Single-Walled Carbon Nanotubes

ARTICLE *in* THE JOURNAL OF PHYSICAL CHEMISTRY C · APRIL 2007

Impact Factor: 4.77 · DOI: 10.1021/jp066469j

4 AUTHORS, INCLUDING:

Tandabany C. Dinadayalane
Clark Atlanta University
66 PUBLICATIONS **1,156** CITATIONS
SEE PROFILE

Anna Kaczmarek-Kedziera
Nicolaus Copernicus University
31 PUBLICATIONS **522** CITATIONS
SEE PROFILE

Jerzy P Lukaszewicz
Nicolaus Copernicus University
103 PUBLICATIONS **454** CITATIONS
SEE PROFILE

Chemisorption of Hydrogen Atoms on the Sidewalls of Armchair Single-Walled Carbon Nanotubes

T. C. Dinadayalane,[†] Anna Kaczmarek,[†,‡] Jerzy Łukaszewicz,[‡] and Jerzy Leszczynski*[,†]

Computational Center for Molecular Structure and Interactions, Department of Chemistry, P.O. Box 17910, Jackson State University, Jackson, Mississippi 39217, and Department of General Chemistry, Nicolaus Copernicus University, 7, Gagarin Street, 87-100 Toruń, Poland

Received: October 2, 2006; In Final Form: January 12, 2007

A computational study using the B3LYP/6-31G(d) level of theory shows that the chemisorptions of one and two hydrogen atoms on the external surface of (3,3), (4,4), (5,5), and (6,6) armchair single-walled carbon nanotubes (SWNTs) are exothermic processes. Our results clearly indicate that two hydrogen atoms favor binding at adjacent positions rather than at alternate carbon sites. This is different from the results reported on zigzag nanotubes (Yang et al. *J. Phys. Chem. B* **2006**, *110*, 6236). In general, the exothermicity of hydrogen chemisorption decreases as the diameter of the armchair nanotubes increases, which is in contrast to the observation for zigzag-type structures. The chemisorptions of one and two hydrogen atoms significantly alter the C−C bond lengths of the nanotube in the vicinity of hydrogen addition as a result of a change in hybridization of the carbon atom(s) at the chemisorption site(s) from sp^2 to sp^3. The effect of increasing the length of the SWNTs on the geometries and the reaction energies of hydrogen chemisorption has also been explored.

Introduction

Single-walled carbon nanotubes (SWNTs) have intrigued many research groups because of their phenomenal electronic and mechanical properties and the variety of potential applications from chemistry and materials science to biomedicine.[1−7] The shapes and unique properties of SWNTs make them noteworthy as a medium for hydrogen storage. Many experimental and theoretical groups have investigated the use of SWNTs as a material for the safe and effective storage of hydrogen.[8−24] Controversy still remains on the hydrogen storage capacities of carbon nanotubes[9−17] since Dillon et al. first measured the hydrogen storage capacity of SWNTs using temperature-programmed desorption (TPD) spectroscopy.[8] Researchers continue their attempts at utilizing various forms of carbon nanotubes,[14−24] activated carbon, and graphite nanofibers,[25−36] which are regarded as attractive substrates for the storage of hydrogen, to achieve the 6.5 wt % target set by the U.S. Department of Energy.

Hydrogen can interact with nanotubes by two different mechanisms: physisorption and chemisorption.[18−20] In the physisorption process, H_2 retains its molecular identity when it interacts with the carbon nanotubes, whereas atomic hydrogen, generated by dissociation of H_2 molecules, binds with the carbon atoms of the nanotubes leading to strong C−H bonds in the chemisorption process. Covalent binding of atomic hydrogen on the sidewalls of SWNTs results in the disruption of the bonding network by changing the carbon atom hybridization from sp^2 to sp^3. In contrast, the aromatic bonding framework is not altered during physisorption. Previously, the physisorption process was suggested to be the principal mechanism for hydrogen storage in carbon nanotubes in the absence of doped catalysts.[10,11,37,38] Compared to theoretical studies on the physisorption of H_2 on SWNTs, investigations involving the chemisorption of hydrogen atoms are limited.[18−21]

Khare et al. reported that atomic hydrogen covalently binds with the carbon atoms of nanotubes and they found evidence of C−H bond formation from their IR stretching modes.[9] Their experimental report stimulated some computational studies on hydrogen chemisorption on the sidewalls of SWNTs.[18−21] Very recently, Dai and co-workers revealed the hydrogenation of SWNTs by means of H-plasma treatment.[39] They observed an increase in the topological height of nanotubes in atomic force microscopy (AFM) images after hydrogenation. Furthermore, they verified hydrogen chemisorption using a vibrational frequency of 2920 cm^{-1} corresponding to sp^3 C−H stretching or asymmetric stretching of sp^3 CH_2 groups. Their experimental investigation showed that the dehydrogenation process is initiated at a temperature of ∼200 °C and is completed at ∼500 °C.[39]

On the basis of density functional theory (DFT) calculations, Lee et al. proposed that the adsorption of hydrogen on SWNTs is a chemisorption process, and their predicted hydrogen storage capacity was more than 14 wt %.[40] Very recently, Yang et al. emphasized the importance of investigating the chemisorption of hydrogen at low occupancies (i.e., binding of one and two hydrogen atoms) on SWNTs.[41] They pointed out that the binding energy of a H atom depends on the H occupancy, the tube diameter, and the chirality. Moreover, they found that exohedral binding of H is more favorable than endohedral binding because of the easier conversion of sp^2 to sp^3 hybridization upon H binding for carbon atoms of the exterior walls.[41] It is important to mention that the chemisorption of H atoms with low occupancy (two and four hydrogen atoms) on single-layer graphene structures was investigated by Zhu et al., who explored

* To whom correspondence should be addressed. E-mail: jerzy@ccmsi.us.
[†] Jackson State University.
[‡] Nicolaus Copernicus University.

10.1021/jp066469j CCC: $37.00
Published on Web 04/27/2007

CHART 1

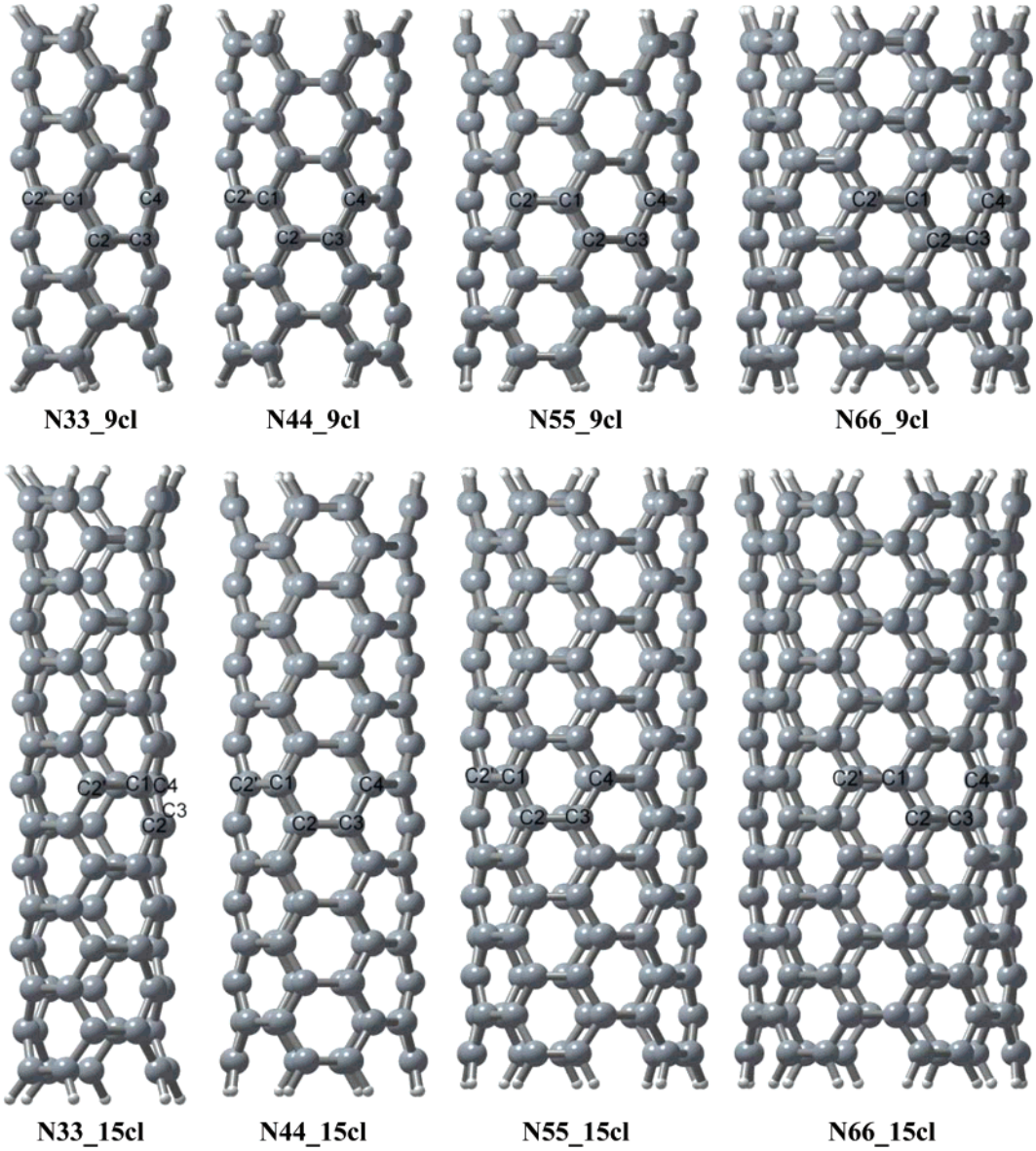

the influence of boron substitution in carbon materials for the improvement of hydrogen atom adsorption.[42]

Small-diameter nanotubes have attracted much attention recently because of their high curvature, leading to properties different from those of large-diameter SWNTs.[43−46] Physisorption of hydrogen on the small-diameter armchair (3,3) and (4,4) SWNTs has been investigated using quantum chemical calculations.[47] However, to our knowledge, studies on the chemisorption of hydrogen atoms on the external surface of these nanotubes have not been reported.

In this article, we report an investigation of the chemisorption of a single hydrogen atom and of the preference for binding positions (i.e., 1−2, 1−2′, 1−3, or 1−4 positions) in the chemisorption of two hydrogen atoms considering (3,3), (4,4), (5,5), and (6,6) armchair SWNTs of 9- and 15-carbon-atom layers (Chart 1). The addition of H atoms only on the outer wall of SWNT (exohedral addition) is considered here because it has been reported to be more favorable than addition on the inner wall of SWNT (endohedral addition).[41] We aim to address the following questions: (a) Do armchair and zigzag nanotubes exhibit same positional preference for the attachment of two hydrogen atoms? (b) How does the diameter of the nanotube affect hydrogen atom chemisorption energies? (c) Does the length of the tube affect the structures and chemisorption energies when one and two hydrogen atoms are attached on the sidewalls of armchair nanotubes?

Computational and Technical Details

Modeling of the chemisorption process, which involves the attachment of one and two hydrogen atoms to carbon atoms of the external surface of (3,3), (4,4), (5,5), and (6,6) armchair nanotubes, was performed within the density functional theory (DFT) framework using the B3LYP functional[48] in conjunction with the 6-31G(d) basis set. To examine the effect of tube length on chemisorption energy, two different lengths were chosen for each of the above-mentioned armchair nanotubes, as shown in Chart 1. The edges of the nanotubes were terminated by hydrogen atoms. In Chart 1, the atom numbers given in the structures indicate the positions where H atoms were attached. A single hydrogen atom was added at C1. Two hydrogen atoms were added simultaneously at the 1−2, 1−2′, 1−3, and 1−4 positions for each of the structures. To determine the nature of the stationary points, we performed frequency calculations for the optimized geometries of the (3,3) and (4,4) SWNTs of 9

carbon layers and their hydrogen-chemisorbed structures. The frequency calculations for larger systems are computationally prohibitive; hence, they were not performed. All calculations were carried out using the Gaussian 03 suite of programs.[49] The reaction energies for hydrogen chemisorption (E_r) on the external surface of the SWNTs were calculated using the equation

$$E_r = E_{SWNT+nH} - E_{SWNT} - nE_H \quad (1)$$

where $E_{SWNT+nH}$ denotes the total energy of the hydrogen-chemisorbed nanotube; n represents the number of hydrogen atoms chemisorbed; and E_{SWNT} and E_H correspond to the energies of the pristine nanotube and the hydrogen atom, respectively. The reaction energy E_r can also be considered as the hydrogen chemisorption energy. The chemisorption of hydrogen is an exothermic process if the value of E_r is negative. The maximum of two hydrogen atoms was considered for chemisorption on SWNTs; thus, the reaction energy per hydrogen atom (E_r/H) addition was calculated as $E_r/2$ in the case of chemisorption of two H atoms.

Results and Discussion

The details of the nomenclature used in this article are given here. The designations **N33**, **N44**, **N55**, and **N66** are used to represent (3,3), (4,4), (5,5), and (6,6) nanotubes, respectively. In these SWNTs, different lengths of nanotubes are denoted by the number of carbon layers; thus, **9cl** and **15cl** correspond to 9 and 15 carbon layers of SWNTs (counted in the axial direction). The positions where hydrogen atoms have been attached on the sidewalls are designated by numbers in parentheses next to H; for instance, H(1,2) indicates that two hydrogen atoms have been chemisorbed to atoms C1 and C2 of the nanotube structures. The B3LYP/6-31G(d)-optimized structures of hydrogen-chemisorbed nanotubes containing 15 carbon layers are depicted in Figure 1, and those of hydrogen-chemisorbed nanotubes containing 9 carbon layers are given in the Supporting Information.

Geometrical Changes upon Hydrogen Addition. Four important bond distances, namely, C1−C2′, C1−C2, C2−C3, and C3−C4 (which are in the hydrogen chemisorption region), for the pristine and H-chemisorbed nanotubes at the B3LYP/6-31G(d) level are listed in Table 1. The above-mentioned bonds are shown in Chart 1 and Figure 1. The data provided in Table 1 indicate that the chemisorptions of one and two hydrogen atoms significantly alter the C−C bond lengths of the nanotube in the vicinity of hydrogen addition. This is due to the change in hybridization of the carbon atom(s) from sp^2 to sp^3 at the chemisorption site(s). The majority of the bond distances decrease in going from (3,3) to (6,6) H-chemisorbed nanotubes. The bond lengths of bare SWNTs range from 1.41 to 1.46 Å. A critical analysis of the data given in Table 1 shows that, for hydrogen-chemisorbed nanotubes, many of the bond distances are longer than 1.5 Å, which represents a typical bond length of sp^2-sp^3 C−C single bonds. This indicates weakening of the C−C bonds in the region of hydrogen chemisorption. The weakening of C−C bonds in hydrogen-chemisorbed nanotubes is much higher in the (3,3) smaller-diameter nanotube compared to the larger-diameter (5,5) and (6,6) SWNTs.

A significant difference in bond lengths is observed between bare and hydrogen-chemisorbed (3,3) tubes compared to larger-diameter (5,5) and (6,6) nanotubes because of the high curvature of (3,3) SWNTs. Some of the C−C bond distances, particularly the C2−C3 bond length of H(1,4)-chemisorbed nanotubes, are less than 1.4 Å, signifying double-bond character. The bond lengths of newly formed C−H bonds in the H-chemisorbed nanotubes are ∼1.1 Å. A perusal of the data collected in Table 1 shows that a significant elongation of the C1−C2′ bond occurred when two hydrogen atoms were added to the nearest-neighbor positions C1 and C2′ [i.e., H(1,2′) addition]. It should be noted that the C1−C2′ bond is of the circumferential type. Although two hydrogen atoms were added to the adjacent carbon sites in H(1,2′) and H(1,2) additions, the elongation of the C1−C2′ bond (bond length is greater than 1.6 Å) is substantially higher in the H(1,2′) hydrogen-chemisorbed SWNTs than the elongation of the C1−C2 bond (bond length is 1.57 Å) in the H(1,2) hydrogen-chemisorbed nanotubes.

The C1−C2′ bond length in **N33_15cl_H(1,2′)** is 2.697 Å, whereas it is 1.67 Å in **N33_9cl_H(1,2′)**. This is surprising because the C1−C2′ bond ruptured in the longer tube, i.e., 15-carbon-layered (3,3) SWNT upon addition of two hydrogen atoms at the C1 and C2′ positions, but it is elongated to a large extent in the 9-carbon-layered (3,3) tube. To understand this bond rupture behavior in the strained large-curvature (3,3) SWNTs, we performed further calculations considering other circumferential bond positions. The optimized geometries of two-hydrogen chemisorption on other circumferential bonds, i.e., H(1,2′) addition in 9 and 15-carbon-layered (3,3) SWNTs, are depicted in Figure 2. As shown in Figure 2, bond rupture also occurred in **N33_9cl_H(1,2′)a**, which is a 9-carbon-layered tube, similar to **N33_15cl_H(1,2′)**. Note that, in both cases, the corresponding bond length in the bare nanotube is ∼ 1.47 Å, which is longer than a typical aromatic C−C double bond. It is important to mention that the bond rupture does not take place when two-hydrogen chemisorption is involved at different locations of a C−C circumferential bond other than the one at the middle of the 15-carbon-layered (3,3) SWNT. However, the length of the bond is significantly elongated upon the chemisorption of two hydrogen atoms. The reason for bond breaking of a particular circumferential C−C bond in a (3,3) SWNT upon the chemisorption of two hydrogen atoms might be the release of the local strain existing at that region of the SWNTs. In structural aspects, the small-diameter (3,3) nanotube behaves differently from the larger-diameter nanotubes considered in this study because the changes in bond length are significantly higher in the former upon hydrogen chemisorption.

A theoretical study by Arellano et al. showed the scission of a circumferential-type C−C bond upon chemisorption of hydrogen atoms, based on molecular dynamics simulations using the local density approximation. They reported a distance of 3.05 Å between the two nearest-neighbor carbon atoms to which the H atoms were bonded.[20] This sort of bond cleavage has been well documented for the addition of CH_2 and O to the circumferential C−C bond of armchair SWNTs.[50−52] It is worth mentioning that the additions of CH_2, SiH_2, NH, and O to the circumferential C−C bond of SWNTs result in elongation of those C−C bonds to more than 2.0 Å.[50−52]

Reaction Energies of Hydrogen Chemisorption. The reaction energies computed at the B3LYP/6-31G(d) level for the chemisorptions of one and two hydrogen atoms on the sidewalls of (3,3), (4,4), (5,5), and (6,6) armchair single-walled carbon nanotubes of 9 and 15 carbon layers and the reaction energies per hydrogen atom addition (E_r/H) are listed in Table 2. The data collected in Table 2 indicate that the reactions of one and two hydrogen atoms on the surface of these armchair nanotubes are highly exothermic. The exothermicity for the addition of two H atoms is more than 2 times that of the addition of one H atom except for H(1,3) addition.

Figure 3 depicts the changes in reaction exothermicity for the chemisorption of one and two hydrogen atoms on the surface

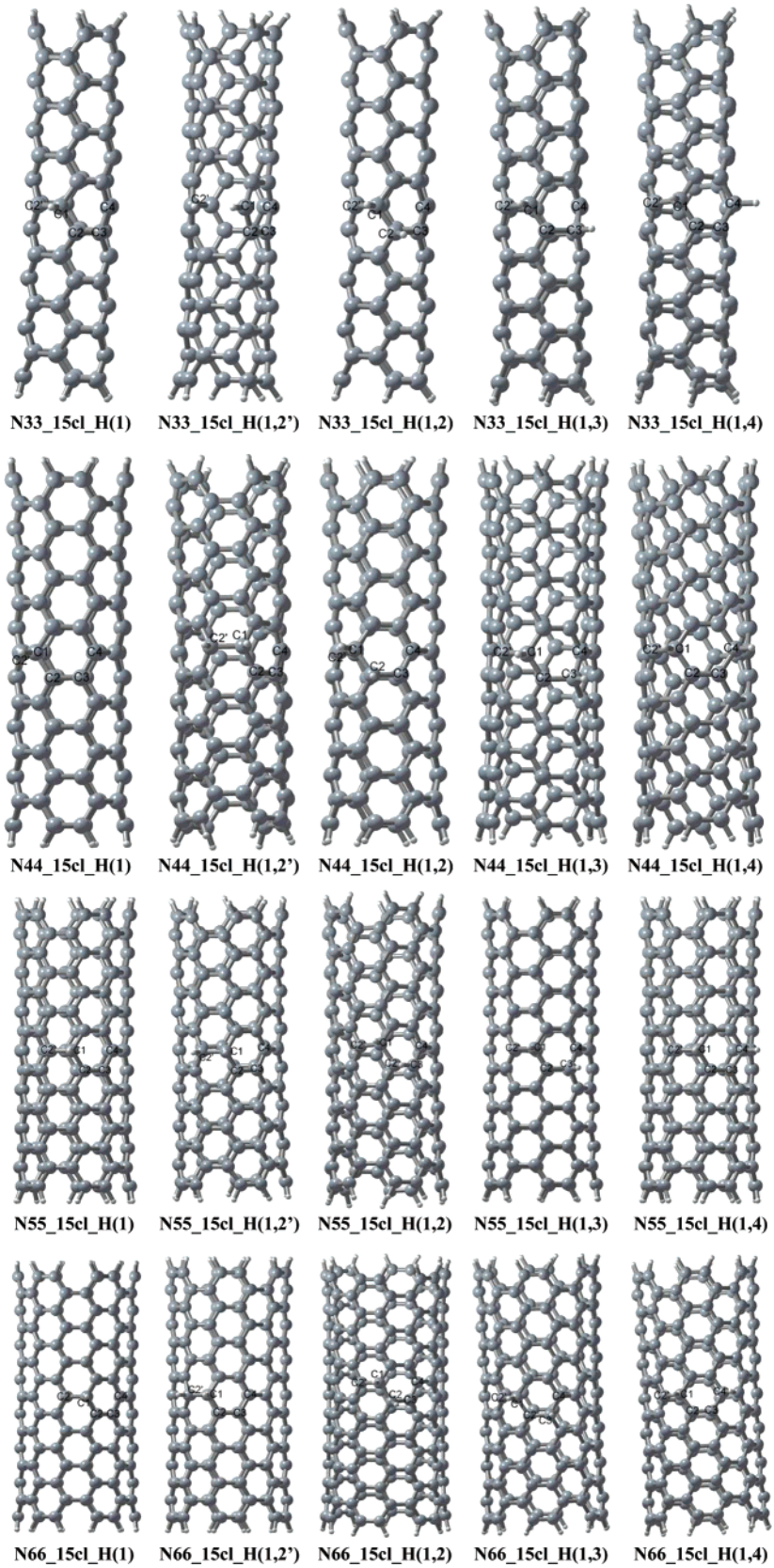

Figure 1. B3LYP/6-31G(d)-optimized structures of hydrogen-chemisorbed (3,3), (4,4), (5,5), and (6,6) armchiar nanotubes of 15 carbon layers (the structures for 9 carbon layers are given in the Supporting Information). The carbon atom positions involved in the attachment of hydrogen atoms are shown in the structures. The gray (large) and white (small) balls correspond to carbon and hydrogen atoms, respectively.

of armchair nanotubes of varying diameters considered in this study. Clearly, the reaction exothermicity is substantially higher in the 15-carbon-layered tubes compared to 9-carbon-layered (3,3) SWNTs. We can see a similar trend between 9- and 15-carbon-layered (5,5) and (6,6) tubes. There is a competition between H(1,2) and H(1,4) addition in the case of (5,5) and

TABLE 1: Important Bond Lengths (in Å) Obtained at the B3LYP/6-31G(d) Level for Hydrogen-Chemisorbed and Pristine (3,3), (4,4), (5,5), and (6,6) SWNTs of 9 and 15 Carbon Layers[a]

	9 carbon layers					15 carbon layers			
	C1−C2′	C1−C2	C2−C3	C3−C4		C1−C2′	C1−C2	C2−C3	C3−C4
				(3,3) SWNT					
N33_9cl	1.413	1.445	1.449	1.445	**N33_15cl**	1.464	1.426	1.430	1.426
H(1)	1.558	1.522	1.413	1.447	**H(1)**	1.561	1.521	1.417	1.446
H(1,2′)	1.669	1.503	1.413	1.449	**H(1,2′)**	2.697	1.400	1.421	1.423
H(1,2)	1.547	1.569	1.548	1.405	**H(1,2)**	1.553	1.572	1.552	1.390
H(1,3)	1.555	1.521	1.563	1.513	**H(1,3)**	1.564	1.516	1.565	1.512
H(1,4)	1.564	1.521	1.380	1.521	**H(1,4)**	1.570	1.516	1.360	1.516
				(4,4) SWNT					
N44_9cl	1.409	1.440	1.427	1.440	**N44_15cl**	1.417	1.437	1.434	1.437
H(1)	1.542	1.521	1.399	1.445	**H(1)**	1.545	1.520	1.406	1.445
H(1,2′)	1.628	1.508	1.400	1.446	**H(1,2′)**	1.641	1.507	1.408	1.445
H(1,2)	1.535	1.569	1.534	1.384	**H(1,2)**	1.536	1.569	1.537	1.406
H(1,3)	1.537	1.517	1.539	1.520	**H(1,3)**	1.540	1.519	1.546	1.521
H(1,4)	1.541	1.517	1.372	1.517	**H(1,4)**	1.546	1.517	1.376	1.517
				(5,5) SWNT					
N55_9cl	1.446	1.418	1.423	1.418	**N55_15cl**	1.416	1.435	1.428	1.435
H(1)	1.534	1.518	1.396	1.443	**H(1)**	1.538	1.519	1.403	1.444
H(1,2′)	1.611	1.510	1.397	1.445	**H(1,2′)**	1.625	1.510	1.406	1.444
H(1,2)	1.527	1.564	1.526	1.380	**H(1,2)**	1.532	1.567	1.532	1.388
H(1,3)	1.531	1.509	1.526	1.521	**H(1,3)**	1.535	1.516	1.538	1.524
H(1,4)	1.534	1.517	1.369	1.517	**H(1,4)**	1.539	1.517	1.376	1.517
				(6,6) SWNT					
N66_9cl	1.440	1.418	1.421	1.418	**N66_15cl**	1.417	1.433	1.425	1.433
H(1)	1.529	1.515	1.395	1.441	**H(1)**	1.534	1.517	1.403	1.443
H(1,2′)	1.600	1.511	1.395	1.444	**H(1,2′)**	1.615	1.511	1.405	1.443
H(1,2)	1.524	1.564	1.524	1.400	**H(1,2)**	1.530	1.567	1.530	1.388
H(1,3)	1.525	1.503	1.522	1.522	**H(1,3)**	1.531	1.510	1.531	1.525
H(1,4)	1.529	1.516	1.369	1.516	**H(1,4)**	1.535	1.517	1.375	1.517

[a] See Figure 1 and text for atom numbers and explanation for symbols.

TABLE 2: Reaction Energies (E_r, kcal/mol) and Reaction Energies Per Hydrogen Atom (E_r/H, kcal/mol) for Hydrogen Chemisorption Reactions on the Sidewalls of (3,3), (4,4), (5,5), and (6,6) SWNTs of 9 and 15 Carbon Layers Calculated at the B3LYP/6-31G(d) Level of Theory

	9 carbon layers			15 carbon layers	
addition site	E_r	E_r/H	addition site	E_r	E_r/H
		(3,3) SWNT			
H(1)	−53.5	−53.5	H(1)	−62.2	−62.2
H(1,2′)	−129.8	−64.9	H(1,2′)	−147.8	−73.9
H(1,2)	−131.4	−65.7	H(1,2)	−139.3	−69.7
H(1,3)	−93.6	−46.8	H(1,3)	−101.9	−50.9
H(1,4)	−114.0	−57.0	H(1,4)	−132.9	−66.5
		(4,4) SWNT			
H(1)	−52.0	−52.0	H(1)	−47.8	−47.8
H(1,2′)	−115.7	−57.9	H(1,2′)	−111.9	−55.9
H(1,2)	−107.2	−53.6	H(1,2)	−108.9	−54.5
H(1,3)	−78.3	−39.1	H(1,3)	−76.5	−38.2
H(1,4)	−115.2	−57.6	H(1,4)	−105.8	−52.9
		(5,5) SWNT			
H(1)	−47.0	−47.0	H(1)	−47.3	−47.3
H(1,2′)	−100.0	−50.0	H(1,2′)	−102.4	−51.2
H(1,2)	−109.3	−54.6	H(1,2)	−105.4	−52.7
H(1,3)	−68.7	−34.3	H(1,3)	−70.8	−35.4
H(1,4)	−110.0	−55.0	H(1,4)	−104.6	−52.3
		(6,6) SWNT			
H(1)	−38.8	−38.8	H(1)	−44.8	−44.8
H(1,2′)	−84.2	−42.1	H(1,2′)	−95.9	−47.9
H(1,2)	−100.6	−50.3	H(1,2)	−103.7	−51.8
H(1,3)	−58.0	−29.0	H(1,3)	−66.1	−33.0
H(1,4)	−101.5	−50.8	H(1,4)	−103.9	−51.9

(6,6) SWNTs, but such competition is not observed in the case of smaller-diameter (3,3) and (4,4) nanotubes. It is important to note that smaller-diameter tubes such as (3,3) and (4,4) do not follow the exact trend of larger-diameter tubes such as (5,5) and (6,6). In the case of 9-carbon-layered tubes, a marked deviation in reaction exothermicity is seen in going from (5,5) to (6,6) SWNTs, whereas the deviation is less significant in the case of 15-carbon-layered tubes. Thus, increasing the length of the tube has a pronounced effect on the reaction exothermicity of hydrogen chemisorption.

Tube diameter has a significant influence on the reaction energy of hydrogen chemisorption. Figure 3 shows that the reaction energy for hydrogen chemisorption on the surface of small-diameter (3,3) nanotubes is much higher than those for the relatively larger-diameter (4,4), (5,5), and (6,6) nanotubes.

TABLE 3: Important Vibrational Frequencies (ν, cm^{-1}) for Hydrogen-Chemisorbed (3,3) and (4,4) SWNTs of 9 Carbon Layers[a,b]

structure	ν (cm^{-1})	vibrational mode
N33_H(1)	2893.3 (17.8)	C−H stretching
N33_H(1,2′)	2949.1 (2.4)	C−H asymmetric stretching
	2967.6 (17.9)	C−H symmetric stretching
N33_H(1,2)	2901.1 (5.6)	C−H asymmetric stretching
	2915.8 (52.1)	C−H symmetric stretching
N33_H(1,3)	2837.0 (36.1)	C1−H stretching
	2854.6 (47.6)	C3−H stretching
N33_H(1,4)	2880.3 (25.2)	C−H asymmetric stretching
	2880.6 (35.9)	C−H symmetric stretching
N44_H(1)	2854.1 (25.4)	C−H stretching
N44_H(1,2′)	2894.8 (3.2)	C−H asymmetric stretching
	2913.4 (32.5)	C−H symmetric stretching
N44_H(1,2)	2875.8 (10.0)	C−H asymmetric stretching
	2897.4 (42.5)	C−H symmetric stretching
N44_H(1,3)	2782.8 (94.8)	C3−H stretching
	2806.9 (48.4)	C1−H stretching
N44_H(1,4)	2852.7 (44.5)	C−H symmetric stretching
	2852.8 (14.9)	C−H asymmetric stretching

[a] Vibrational frequencies were scaled with a scaling factor of 0.9614 (ref 54). [b] IR intensities (in km/mol) are given in parentheses.

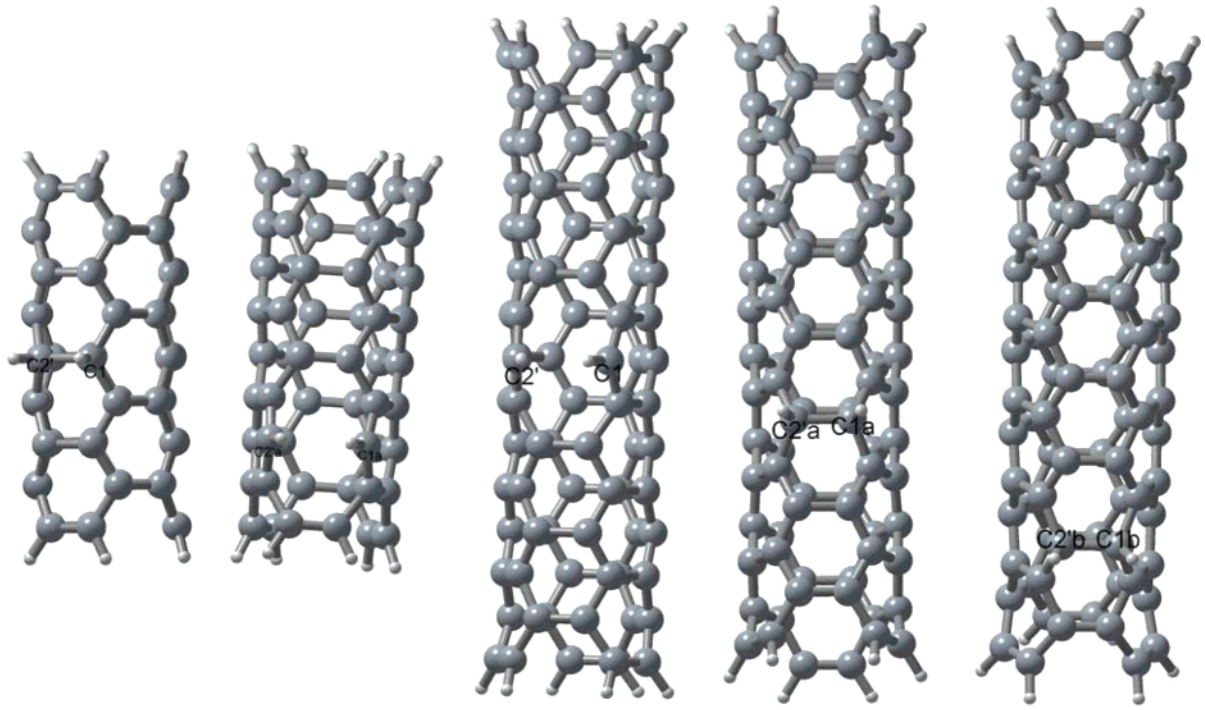

Figure 2. B3LYP/6-31G(d)-optimized geometries of H(1,2′) addition of two hydrogen atoms at various circumferential bond positions of (3,3) SWNTs. The C1−C2′ bond distances (in Å) for the hydrogen-chemisorbed tubes, the corresponding values for bare nanotubes (given in parentheses), and the reaction exothermicities (E_r, in kcal/mol) for hydrogen chemisorptions are given.

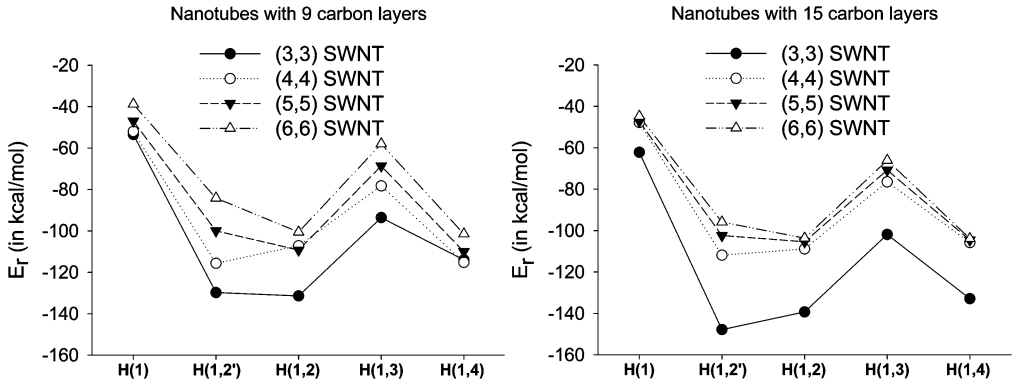

Figure 3. Variation of reaction energies at the B3LYP/6-31G(d) level for the chemisorption of one and two hydrogen atoms on the external surface of (3,3), (4,4), (5,5), and (6,6) armchair single-walled carbon nanotubes (SWNTs).

This can be ascribed to the large curvature of (3,3) SWNTs. Large curvature facilitates the transition from sp^2 to sp^3 carbon hybridization upon hydrogen addition. The results of molecular dynamics simulations reported by Cheng et al. indicate that the heat of physisorption of a H_2 molecule increases as the nanotube diameter decreases for both armchair and zigzag nanotubes.[23] Hence, we address here the issue of how the reaction exothermicity of hydrogen chemisorption varies as the tube diameter changes in both zigzag- and armchair-type nanotubes. A critical examination of the values displayed in Table 2 shows that the exothermicity of hydrogen chemisorption decreases in going from (3,3) to (6,6) nanotubes of 15 carbon layers, but there are two exceptions, as seen in Figure 3, for nanotubes with 9 carbon layers. This situation is opposite to that for zigzag-type SWNTs; Yang et al. recently reported an increase in the reaction exothermicity of hydrogen chemisorption when going from smaller- to larger-diameter zigzag SWNTs.[41] Thus, interestingly, the trend in exothermicity of hydrogen chemisorption with changing nanotube diameter is different for armchair- and zigzag-type structures.

Figure 3 shows that the addition of H(1,3) is thermodynamically less favored than the H(1,2) and H(1,2′) additions regardless of the length and diameter of the SWNTs considered. The least positional preference of H(1,3) for armchair SWNTs is different from the results reported recently for zigzag-type nanotubes by Yang et al.[41] Similar to zigzag models, the attachment of two hydrogen atoms at adjacent carbon positions is less favored than that at two alternate carbon sites in the case of graphene sheets.[41] The thermodynamically lower preference for adjacent positions compared to alternate carbon sites for

the chemisorption of two hydrogen atoms on zigzag tubes and graphene sheets was attributed to the "crowding effect" by Yang et al.,[41] but the results obtained in the present study for armchair nanotubes fail to support the reason of the crowding effect. Lee and co-workers revealed that addition at ortho (1,2) positions is more favored than addition at meta (1,3) and para (1,4) positions for both armchair and zigzag nanotubes when two NO_2 groups are attached to the sidewalls.[53] Such consistency of positional preference for the chemisorption of two hydrogen atoms is not obtained between armchair- and zigzag-type nanotubes.

The reaction energies for the chemisorption of two hydrogen atoms at various circumferential bond positions in (3,3) nanotubes are given in Figure 2. It is clear that the exothermicity is substantially higher for nanotubes undergoing bond rupture than for structures obtained without complete bond breaking. Thus, in two-hydrogen chemisorption, the nanotubes with ruptured C−C bonds are more stable than the nanotubes of the same length without broken bonds (Figure 2). Such an observation was already reported by Chen et al. for addition reactions with SWNTs.[50]

Vibrational Frequencies. The important vibrational frequencies of hydrogen-chemisorbed (3,3) and (4,4) nanotubes with 9 carbon layers are listed in Table 3. The reported vibrational frequencies in Table 3 were scaled by a factor of 0.9614 as suggested by Scott and Radom.[53] The frequency calculations for larger systems are computationally prohibitive; hence, such calculations were not performed. The vibrational frequency analysis for the structures of hydrogen-chemisorbed nanotubes of smaller-diameter [(3,3) and (4,4) SWNTs] with 9 carbon layers indicates that the structures are minima on the potential energy surface. The values of C−H stretching frequencies for chemisorbed hydrogens are lower for (4,4) than (3,3) SWNTs. The vibrational frequency data reveal that hydrogen chemisorption on nanotubes of different diameters and the positions of two hydrogen atoms chemisorbed on the surface of armchair SWNTs can be characterized by stretching frequency values. The C−H stretching frequencies of H(1,3)- and H(1,4)-chemisorbed nanotubes are lower than those for single-hydrogen-chemisorbed SWNTs for both (3,3) and (4,4). Thermodynamically least stable H(1,3)-chemisorbed SWNTs exhibit lower values of C−H stretching frequencies than the other dihydrogen-chemisorbed nanotubes considered in this study. It is important to note that the stretching of the two C−H bonds is coupled symmetrically as well as asymmetrically in H(1,2)-, H(1,2′)-, and H(1,4)-chemisorbed structures. There is no coupling of these two C−H bonds stretching in H(1,3)-chemisorbed SWNTs.

Conclusions

Density functional theory, B3LYP/6-31G(d) calculations have been performed to examine the structures and reaction energies resulting from the chemisorption of one and two hydrogen atoms on the exterior surface of (3,3), (4,4), (5,5), and (6,6) armchair nanotubes. Chemisorption of one and two hydrogen atoms alters the bond lengths in the vicinity of the addition sites. Our results show that the exothermicity of hydrogen chemisorption decreases as the diameter of the armchair nanotubes increases. This is different from the trend obtained for zigzag SWNTs.[41] The present study indicates that two hydrogen atoms prefer to bind at adjacent positions compared to alternate carbon sites of armchair nanotubes. This does not support the reason of the crowding effect given by Yang et al. for the lower binding energy of 1,2- compared to 1,3-addition of two hydrogen atoms.[41] Armchair and zigzag nanotubes do not exhibit the same positional preference for the attachment of two hydrogen atoms. However, in the case of binding of two NO_2 groups on SWNT sidewalls, ortho (1,2) addition is more favorable than meta (1,3) and para (1,4) addition for both armchair and zigzag nanotubes.[53] Changing the length of the nanotube has a significant effect on the reaction energy of hydrogen chemisorption. The present study will be helpful in elucidating the chemisorption of spillover hydrogen atoms on the surface of armchair nanotubes and might enhance the experimental interest in hydrogen chemisorption of low occupancy on the sidewalls of small-diameter nanotubes.

Acknowledgment. This research was supported by the U.S. Army Engineer Research and Development Center, Grant W912HZ-05-C-0051, the High Performance Computational Design of Novel Materials (HPCDNM) Project funded by the Department of Defense through the U.S. Army Engineer Research and Development Center (Vicksburg, MS), Contract W912HZ-06-C-0057, and the Office of Naval Research (ONR), Grant N00014-03-1-0116. The Mississippi Center for Supercomputing Research (MCSR) and the Army High Performance Computing Research Center (AHPCRC) are acknowledged for computational facilities.

Supporting Information Available: B3LYP/6-31G(d)-optimized structures of 9- and 15-carbon-layered hydrogen-chemisorbed and pristine nanotubes and total energies for pristine and hydrogen-chemisorbed nanotubes considered in this study. This material is available free of charge via the Internet at http://pubs.acs.org.

References and Notes

(1) Iijima, S.; Ichihashi, T. *Nature* **1993**, *363*, 603.
(2) Baughman, R. H.; Zakhidov, A. A.; de Heer, W. A. *Science* **2002**, *297*, 787.
(3) Saito, R.; Dresselhaus, M. S.; Dresselhaus, G. *Physical Properties of Carbon Nanotubes*; Imperial College Press: London, 1998.
(4) Tasis, D.; Tagmatarchis, N.; Bianco, A.; Prato, M. *Chem. Rev.* **2006**, *106*, 1105.
(5) Wu, W.; Wieckowski, S.; Pastorin, G.; Benincasa, M.; Klumpp, C.; Briand, J. -P.; Gennaro, R.; Prato, M.; Bianco, A. *Angew. Chem., Int. Ed.* **2005**, *44*, 6358.
(6) Dinadayalane, T. C.; Leszczynski, J. Toward Nanomaterials: Structural, Energetic and Reactivity Aspects of Single-Walled Carbon Nanotubes. In *Nanomaterials: Design and Simulation*; Balbuena, P. B., Seminario, J. M., Eds.; Elsevier: Amsterdam, 2006; pp 167−199.
(7) Dinadayalane, T. C.; Leszczynski, J. *Chem. Phys. Lett.* **2007**, *434*, 86.
(8) Dillon, A. C.; Jones, K. M.; Bekkedahl, T. A.; Kiang, C. H.; Bethune, D. S.; Heben, M. J. *Nature* **1997**, *386*, 377.
(9) Khare, B. N.; Meyyappan, M.; Casell, A. M.; Nguyen, C. V.; Han, J. *Nano Lett.* **2002**, *2*, 73.
(10) Nikitin, A.; Ogasawara, H.; Mann, D.; Denecke, R.; Zhang, Z.; Dai, H.; Cho, K.; Nilsson, A. *Phys. Rev. Lett.* **2005**, *95*, 225507.
(11) Ye, Y.; Ahn, C. C.; Witham, C.; Fultz, B.; Liu, J.; Rinzler, A. G.; Collbert, D.; Smith, K. A.; Smalley, R. E. *Appl. Phys. Lett.* **1999**, *74*, 2307.
(12) Liu, C.; Fan, Y. Y.; Liu, M.; Cong, H. T.; Cheng, H. M.; Dresselhaus, M. S. *Science* **1999**, *286*, 1127.
(13) Chen, P.; Wu, X.; Lin, J.; Tan, K. L. *Science* **1999**, *285*, 91.
(14) Wang, Q.; Johnson, J. K. *J. Phys. Chem. B* **1999**, *103*, 4809.
(15) Sudan, P.; Zuttel, A.; Mauron, Ph.; Emmenegger, Ch.; Wenger, P.; Schlapbach, L. *Carbon* **2003**, *41*, 2377.
(16) Gundiah, G.; Govindaraj, A.; Rajalakshmi, N.; Dhathathreyan, K. S.; Rao, C. N. R. *J. Mater. Chem.* **2003**, *13*, 209.
(17) Efremenko, I.; Sheintuch, M. *Langmuir* **2005**, *21*, 6282.
(18) Barone, V.; Heyd, J.; Scuseria, S. E. *J. Chem. Phys.* **2004**, *120*, 7169.
(19) Li, J.; Furuta, T.; Goto, H.; Ohashi, T.; Fujiwara, Y.; Yip, S. *J. Chem. Phys.* **2003**, *119*, 2376.
(20) Arellano, J. S.; Molina, L. M.; Rubio, A.; Lopez, M. J.; Alonso, J. A. *J. Chem. Phys.* **2002**, *117*, 2281.
(21) Bauschlicher C. W., Jr.; So, C. R. *Nano Lett.* **2002**, *2*, 337.
(22) Cabria, I.; Lopez, M. J.; Alonso, J. A. *Comput. Mater. Sci.* **2006**, *35*, 238.

(23) Cheng, H.; Cooper, A. C.; Pez, G. P.; Kostov, M. K.; Piotrowski, P.; Stuart, S. J. *J. Phys. Chem. B* **2005**, *109*, 3780.
(24) Wang, Q.; Johnson, J. K. *J. Chem. Phys.* **1999**, *110*, 577.
(25) Cheng, H.; Pez, G. P.; Cooper, A. C. *J. Am. Chem. Soc*. **2001**, *123*, 5845.
(26) Wang, Q.; Johnson, J. K. *J. Phys. Chem. B* **1999**, *103*, 277.
(27) Meregalli, V.; Parrinello, M. *Appl. Phys. A* **2001**, *72*, 143.
(28) Yang, F. H.; Yang, R. T. *Carbon* **2002**, *40*, 437.
(29) Volpe, M.; Cleri, F. *Surf. Sci*. **2003**, *544*, 24.
(30) Miura, Y.; Kasai, H.; Dino, W.; Nakanishi, H.; Sugimoto, T. *J. Appl. Phys*. **2003**, *93*, 3395.
(31) Patchkovskii, S.; Tse, J. S.; Yurchenko, S. N.; Zhechkov, L.; Heine, T.; Seifert, G. *Proc. Natl. Acad. Sci. U.S.A.* **2005**, *102*, 10439.
(32) Ahn, C. C.; Ye, Y.; Ratnakumar, B. V.; Witham, C.; Bowman, Jr. R. C.; Fultz, B. *Appl. Phys. Lett*. **1998**, *73*, 3378.
(33) Cracknell, R. F. *Phys. Chem. Chem. Phys*. **2001**, *3*, 2091.
(34) Orimo, S.; Majer, G.; Fukunaga, T.; Zuttel, A.; Schlapbach, L.; Fujii, H. *Appl. Phys. Lett*. **1999**, *75*, 3093.
(35) Dino, W. A.; Miura, Y.; Nakanishi, H.; Kasai, H.; Sugimoto, T.; Kondo, T. *Solid State Commun.* **2004**, *132*, 713.
(36) Dino, W. A.; Nakanishi, H.; Kasai, H.; Sugimoto, T.; Kondo, T. *e-J. Surf. Sci. Nanotechnol*. **2004**, *2*, 77.
(37) Kim, H. -S.; Lee, H.; Han, K. -S.; Kim, J. -H.; Song, M. -S.; Park, M. -S.; Lee, J. -Y.; Kang, J. -K. *J. Phys. Chem. B* **2005**, *109*, 8983.
(38) Anson, A.; Lafuente, E.; Urriolabeitia, E.; Navarro, R.; Benito, A. M.; Maser, W. K.; Martinez, M. T. *J. Phys. Chem. B* **2006**, *110*, 6643.
(39) Zhang, G.; Qi, P.; Wang, X.; Lu, Y.; Mann, D.; Li, X.; Dai, H. *J. Am. Chem. Soc*. **2006**, *128*, 6026.
(40) Lee, S. M.; Lee, Y. H. *Phys. Rev. Lett.* **2000**, *76*, 2877.
(41) Yang, F. H.; Lachawiec A. J., Jr.; Yang, R. T. *J. Phys. Chem. B* **2006**, *110*, 6236.
(42) Zhu, Z. H.; Lu, G. Q.; Hatori, H. *J. Phys. Chem. B* **2006**, *110*, 1249.
(43) Wang, W. L.; Bai, X. D.; Xu, Z.; Liu, S.; Wang, E. G. *Chem. Phys. Lett*. **2006**, *419*, 81.
(44) Tan, Y.; Resasco, D. E. *J. Phys. Chem. B* **2005**, *109*, 14454.
(45) Hayashi, T.; Kim, Y. A.; Matoba, T.; Esaka, M.; Nishimura, K.; Tsukada, T.; Endo, M.; Dresselhaus, M. S. *Nano Lett.* **2003**, *3*, 887.
(46) Zhao, X.; Liu, Y.; Inoue, S.; Suzuki, T.; Jones, R. O.; Ando, Y. *Phys. Rev. Lett*. **2004**, *92*, 125502.
(47) Tada, K.; Furuya, S.; Watanabe, K. *Phys. Rev. B* **2001**, *63*, 155405.
(48) (a) Becke, A. D. *J. Chem. Phys.* **1993**, *98*, 5648. (b) Stevens, P. J.; Devlin, F. J.; Chabalowski, C. F.; Frisch, M. J. *J. Phys. Chem.* **1994**, *98*, 11623. (c) Lee, C.; Yang, W.; Parr, R. G. *Phys. Rev. B* **1988**, *37*, 785.
(49) Frisch, M. J. ; Trucks, G. W.; Schlegel, H. B.; Scuseria, G. E.; Robb, M. A.; Cheeseman, J. R.; Montgomery, J. A., Jr.; Vreven, T.; Kudin, K. N.; Burant, J. C.; Millam, J. M.; Iyengar, S. S.; Tomasi, J.; Barone, V.; Mennucci, B.; Cossi, M.; Scalmani, G.; Rega, N.; Petersson, G. A.; Nakatsuji, H.; Hada, M.; Ehara, M.; Toyota, K.; Fukuda, R.; Hasegawa, J.; Ishida, M.; Nakajima, T.; Honda, Y.; Kitao, O.; Nakai, H.; Klene, M.; Li, X.; Knox, J. E.; Hratchian, H. P.; Cross, J. B.; Bakken, V.; Adamo, C.; Jaramillo, J.; Gomperts, R.; Stratmann, R. E.; Yazyev, O.; Austin, A. J.; Cammi, R.; Pomelli, C.; Ochterski, J. W.; Ayala, P. Y.; Morokuma, K.; Voth, G. A.; Salvador, P.; Dannenberg, J. J.; Zakrzewski, V. G.; Dapprich, S.; Daniels, A. D.; Strain, M. C.; Farkas, O.; Malick, D. K.; Rabuck, A. D.; Raghavachari, K.; Foresman, J. B.; Ortiz, J. V.; Cui, Q.; Baboul, A. G.; Clifford, S.; Cioslowski, J.; Stefanov, B. B.; Liu, G.; Liashenko, A.; Piskorz, P.; Komaromi, I.; Martin, R. L.; Fox, D. J.; Keith, T.; Al-Laham, M. A.; Peng, C. Y.; Nanayakkara, A.; Challacombe, M.; Gill, P. M. W.; Johnson, B.; Chen, W.; Wong, M. W.; Gonzalez, C.; Pople, J. A. *Gaussian 03*, revision C.02; Gaussian, Inc.: Wallingford, CT, 2004.
(50) Chen, Z.; Nagase, S.; Hirsch, A.; Haddon, R. C.; Thiel, W.; Schleyer, P. v. R. *Angew. Chem., Int. Ed*. **2004**, *43*, 1552.
(51) Bettinger, H. F. *Chem. Eur. J*. **2006**, *12*, 4372.
(52) Lu, X.; Chen, Z.; Schleyer, P. v. R. *J. Am. Chem. Soc*. **2005**, *127*, 20.
(53) Seo, K.; Park, K. Ah.; Kim, C.; Han, S.; Kim, B.; Lee, Y. H. *J. Am. Chem. Soc*. **2005**, *127*, 15724.
(54) Scott, A. P.; Radom, L. *J. Phys. Chem*. **1996**, *110*, 16502.